Journal of Solid State Chemistry 182 (2009) 905–912

Contents lists available at ScienceDirect

Journal of Solid State Chemistry

journal homepage: www.elsevier.com/locate/jssc

$[Ni(H_2O)_4]_3[U(OH,H_2O)(UO_2)_8O_{12}(OH)_3]$, crystal structure and comparison with uranium minerals with U_3O_8-type sheets

Murielle Rivenet *, Nicolas Vigier, Pascal Roussel, Francis Abraham

Unité de Catalyse et de Chimie du Solide, Equipe Chimie du Solide, UCCS UMR CNRS 8181, USTL, ENSC-B.P. 90108, 59652 Villeneuve d'Ascq Cedex, France

ARTICLE INFO

Article history:
Received 28 October 2008
Received in revised form
14 January 2009
Accepted 16 January 2009
Available online 26 February 2009

Keywords:
Nickel uranium hydroxide
Nickel uranium oxide
U_3O_8-type sheet
Crystal structure

ABSTRACT

The new U(VI) compound, $[Ni(H_2O)_4]_3[U(OH,H_2O)(UO_2)_8O_{12}(OH)_3]$, was synthesized by mild hydrothermal reaction of uranyl and nickel nitrates. The crystal-structure was solved in the P-1 space group, $a = 8.627(2)$, $b = 10.566(2)$, $c = 12.091(4)$ Å and $\alpha = 110.59(1)$, $\beta = 102.96(2)$, $\gamma = 105.50(1)^\circ$, $R = 0.0539$ and w$R = 0.0464$ from 3441 unique observed reflections and 151 parameters. The structure of the title compound is built from sheets of uranium polyhedra closely related to that in β-U_3O_8. Within the sheets $[(UO_2)(OH)O_4]$ pentagonal bipyramids share equatorial edges to form chains, which are cross-linked by $[(UO_2)O_4]$ and $[UO_4(H_2O)(OH)]$ square bipyramids and through hydroxyl groups shared between $[(UO_2)(OH)O_4]$ pentagonal bipyramids. The sheets are pillared by sharing the apical oxygen atoms of the $[(UO_2)(OH)O_4]$ pentagonal bipyramids with the oxygen atoms of $[NiO_2(H_2O)_4]$ octahedral units. That builds a three-dimensional framework with water molecules pointing towards the channels. On heating $[Ni(H_2O)_4]_3[U(OH,H_2O)(UO_2)_8O_{12}(OH)_3]$ decomposes into NiU_3O_{10}.

1. Introduction

These last decades, uranium-containing oxo-hydroxide hydrates have received renewed interest due to their relevance to the long-term storage of spent nuclear fuel. They can be obtained as secondary products of alteration of uraninite ($U^{IV}O_2$) under oxidizing conditions and as primary alteration phases in experimental studies on the oxidative dissolution of UO_2 and of spent nuclear fuel [1–5]. The systematic study of their structural features shows that most of them have a layered structure. Their sheets have a general formula $[U_u(UO_2)_v(CO_3)_pO_x(OH)_y(H_2O)_z]$ in which U can consist in U^{4+}, U^{5+} or U^{6+} and (UO_2) is the uranyl cation, $(U^{VI}O_2)^{2+}$. The electrical charge of the sheets depends on the valences for uranium atoms and on the OH^-/O^{2-} ratio. According to the resulting charge of the inorganic framework, the interlayer space accommodates either for water molecules or for monovalent or divalent cations. One example of oxo-hydroxide hydrate material containing uranium and nickel was reported so far, $NiU_3O_{10}.6H_2O$ [6].

This compound was obtained by adding 100 cm^3 of a $NiSO_4$ solution (0.5 mol dm^{-3}) to 1 g of schoepite, $H_3O[(UO_2)O(OH)]$ [7]. Although no structural determination was being carried out, it was argued that ionic exchanges occur between the H_3O^+ ions of schoepite and the Ni^{2+} cations of solution so as $NiU_3O_{10}.6H_2O$ can be formulated $Ni[(UO_2)_3O_3(OH)_2]\cdot 5H_2O$. Indeed, the structural formula of schoepite, $H_3O[(UO_2)O(OH)]$, on which this hypothesis was based, is disproved by the one recently determined from single-crystal X-ray diffraction data $[(UO_2)_8O_2(OH)_{12}](H_2O)_{12}$ [8]. The latter suggests that the neutral sheets of schoepite, $[(UO_2)_8O_2(OH)_{12}]$, undergo $(OH)^- \leftrightarrow O^{2-}$ substitutions as it is reported in studies on α-U_3O_8 related materials [9–11]. That would allow interstitial H_2O groups to be replaced by Ni^{2+} cations in the interlayer space of schoepite.

The new uranium and nickel oxo-hydroxide hydrate described in the present paper was synthesized by hydrothermal reaction of uranyl nitrate and nickel nitrate in acidic conditions. Crystal structure determination led to the conclusion that the as-obtained compound contains hexavalent uranium U(VI) both as U^{6+} cation and $(UO_2)^{2+}$ uranyl ions. The crystal structure and thermal behavior of the obtained compound are reported herein.

2. Experimental

2.1. Synthesis

Crystals of $[Ni(H_2O)_4]_3[U(OH,H_2O)(UO_2)_8O_{12}(OH)_3]$ were synthesized by mild hydrothermal reaction of uranyl nitrate (0.24 mmol) and nickel nitrate (1 mmol) in distilled water (12 mL). The mixture was acidified by adding oxalic acid (2 mmol) to a pH value of ca. 1, then, heated in a 23 mL Teflon-lined Parr digestion bomb at 180 °C for 7 days. The resulting product was recovered by filtration, washed with water and finally dried in air at room temperature. Optical analysis evidenced that the orange-colored

* Corresponding author. Fax: +33 3 20 43 68 14.
E-mail address: Murielle.rivenet@ensc-lille.fr (M. Rivenet).

0022-4596/$ - see front matter © 2009 Elsevier Inc. All rights reserved.
doi:10.1016/j.jssc.2009.01.019

crystals of $[Ni(H_2O)_4]_3[U(OH,H_2O)(UO_2)_8O_{12}(OH)_3]$ are mixed with a light-blue powder from which they can be isolated using ultrasonics. The role of oxalic acid in the reaction remains unclear since the uranyl cations have a strong affinity for $C_2O_4^{2-}$ anions but no oxalate group was found in the final product. The yield of reaction is estimated at about 20% on the basis of U.

2.2. Characterization

Several crystals were analyzed by energy dispersive spectroscopy using a JEOL JSM-5300 scanning microscope equipped with a PGT digital spectrometer. Analyses confirmed the presence of Ni and U in a ratio close to Ni/U = 1/3.

2.3. Crystal structure determination

For structure determination, a crystal was selected, mounted on a glass fiber and aligned on a BRUKER AXS Apex2 CCD-4K diffractometer system equipped with a Mo-target X-ray tube ($\lambda = 0.71073$ Å) operating at 1500 W power (50 kV, 30 mA). The individual frames were measured using a phi-ω scan strategy. Omega and phi rotations were fixed at 0.5° with an acquisition time of 20 s frame^{-1}. 1630 frames were collected in order to cover the full sphere. Careful examination of the recorded reciprocal space showed that a few reflections could not be indexed using only one domain, suggesting the existence of a twin. Cell-Now software [12] was used to derive the two orientation matrices; it appears that the selected crystal is in fact made from two domains related by a 180° rotation about the −110 reciprocal axis. Intensities were then extracted from collected frames using the program SaintPlus 7.53a [13] taking into account the two domains. After data processing, absorption corrections were performed using a semi-empirical method based on redundancy with the TWINABS program [14]. The resulting set of "HKLF4-untwined" *hkl* was used for structure resolution, while the refinements, performed with the JANA2000 software package [15], were conducted using the twined HKLF5 set of data. Afterward refinements indicate 76.6% of domain 1 and consequently 23.4% of domain 2.

The structure was solved in the centrosymmetric P-1 space group. The final triclinic unit-cell dimensions were refined to $a = 8.627(2)$, $b = 10.566(2)$, $c = 12.091(4)$ Å and $\alpha = 110.59(1)$, $\beta = 102.96(2)$, $\gamma = 105.50(1)°$. Details of the data collection and refinements are summarized in Table 1.

Uranium atoms were located by means of direct methods using SIR97 program [16] although nickel and oxygen atoms were found from successive Fourier difference maps. Refining anisotropic temperature factors for all atoms was tested but it resulted in some non-positive definite values for some oxygen atoms of the structure. This can be attributed to an imperfect absorption correction since the shape of the selected crystal was poorly defined and consequently accurate numerical correction could not be applied. Hence, we decided to refine anisotropic temperature factor for U and Ni atoms and isotropic temperature factors for the oxygen atoms. Hydrogen atoms could not be located as often the case in heavy uranium atoms containing phases. Atomic coordinates with isotropic displacements parameters are given in Table 2. Anisotropic displacements parameters for U and Ni atoms are reported in Table 3.

2.4. Powder characterization

The $[Ni(H_2O)_4]_3[U(OH,H_2O)(UO_2)_8O_{12}(OH)_3]$ powder was obtained by collecting and crushing single-crystals. The X-ray diffraction pattern of the as-obtained powder was recorded with a Bruker AXS D8 ADVANCE diffractometer with the parafocusing Bragg–Brentano geometry, using Cu$K\alpha$1,α2 radiation ($\lambda_{K\alpha1} = 1.54051$ Å, $\lambda_{K\alpha2} = 1.54433$ Å) and an energy dispersive detector (sol-X). The pattern was recorded under air over the angular range 5–70° (2θ), with a step length of 0.02° (2θ) and a counting time of 15 s step^{-1}. Comparison between the powder X-ray diffraction pattern and the theoretical pattern calculated from the crystal structure results evidenced that a pure phase is obtained. The unit cell parameters were refined from the powder pattern by using JANA2000 package [15] leading to $a = 8.6315(2)$, $b = 10.5624(3)$, $c = 12.0954(4)$ Å, $\alpha = 110.666(2)$, $\beta = 102.812(2)$, $\gamma = 105.464(2)°$ values in good agreement with those obtained using the single-crystal data (Table 1).

Temperature-dependent X-ray diffraction pattern was recorded using a Guinier-Lenné moving film camera. The powdered sample was deposited on the sample holder (gold grid) using an ethanol slurry, which yields a regular layer of powdered compound upon evaporation. The high temperature X-ray diffraction pattern was collected in the temperature range [20–1000 °C] with a heating rate of 22° h^{-1}.

Thermal gravimetric analysis and differential thermal analysis (TGA/DTA) were used for investigating the thermal behavior of $[Ni(H_2O)_4]_3[U(OH,H_2O)(UO_2)_8O_{12}(OH)_3]$. Analysis was performed in air, using a Setaram coupled TGA-DTA 2-16.18 apparatus, in the

Table 1
Crystal data and structure refinement for $[Ni(H_2O)_4]_3[U(OH,H_2O)(UO_2)_8O_{12}(OH)_3]$.

Chemical formula	$Ni_3U_9O_{28}(OH)_4(H_2O)_{13}$
Crystallographic data	
Formula weight (g mol^{-1})	3068.5
Crystal system	Triclinic
Space group	*P*-1
Unit-cell dimensions (Å)	$a = 8.627(2)$
	$b = 10.566(2)$
	$c = 12.091(4)$
	$\alpha = 110.59(1)$
	$\beta = 102.96(2)$
	$\gamma = 105.50(1)$
Cell volume (Å^3)	930.3(5)
Z	1
Density, calculated (g cm^{-1})	5.476(2)
F(000)	1272
Intensity collection	
Wavelength (Å)	0.71069 (Mo$K\alpha$)
θ range (°)	1.92–31.74
Data collected	$-12 \leqslant h \leqslant 12$
	$-15 \leqslant k \leqslant 13$
	$0 \leqslant l \leqslant 17$
No. of reflections measured	35347
No. of observed reflections ($I > 3\sigma(I)$)	10450
μ (Mo$K\alpha$) (mm^{-1})	40.621
T_{min}/T_{max}	0.196/0.434
$R(F^2)_{int}$ obs/all	0.0662/0.0998
Refinement	
No. of reflections used	5899
No. of unique reflections ($I > 3\sigma(I)$)	3441
No. of parameters	151
Weighting scheme	$1/\sigma^2$
R(*F*) obs/all	0.0539/0.1205
w *R*(*F*) obs/all	0.0464/0.0509
Max, min $\Delta\rho$ (e. Å^{-3})	7.53/−8.63[a]
Twinning matrices	|−1.000 0.000 0.961|
	|0.000 −1.000 1.014|
	|0.000 0.000 1.000|
Twin volume fraction (domain 1/domain 2)	0.766/0.234

[a] Close to U(5).

Table 2
Atomic coordinates and isotropic (O atoms) or equivalent (U and Ni atoms) displacement parameters (Å^2) for $[Ni(H_2O)_4]_3[U(OH,H_2O)(UO_2)_8O_{12}(OH)_3]$.

Atom	Wyck.	τ	x	y	z	$U_{iso/eq}$
U1	2*i*		0.65669(9)	0.12975(7)	0.65890(6)	0.0072(3)
U2	2*i*		0.02715(9)	0.51314(7)	0.65849(6)	0.0069(3)
U3	2*i*		0.30732(9)	0.80320(7)	0.99866(6)	0.0074(3)
U4	2*i*		0.3169(1)	0.85328(8)	0.67889(7)	0.0079(3)
U5	1*c*		0	0.5	0	0.0342(6)
Ni1	2*i*		0.3721(3)	0.3516(2)	0.6625(2)	0.013(1)
Ni2	1*a*		0	0	0	0.020(2)
O1	2*i*		0.774(2)	0.008(2)	0.660(1)	0.009(2)
O2	2*i*		0.547(2)	0.255(2)	0.661(2)	0.009(2)
O3	2*i*		0.210(2)	0.463(2)	0.663(2)	0.009(2)
O4	2*i*		−0.159(2)	0.561(2)	0.660(2)	0.011(2)
O5	2*i*		0.455(2)	0.705(2)	0.985(2)	0.040(4)
O6	2*i*		0.159(2)	0.894(2)	0.015(2)	0.039(4)
O7	2*i*		0.472(2)	0.756(2)	0.674(2)	0.023(3)
O8	2*i*		0.170(2)	0.952(2)	0.691(2)	0.024(3)
O9	2*i*		0.398(2)	0.936(2)	0.549(1)	0.007(2)
O10	2*i*		0.540(2)	0.064(2)	0.797(2)	0.012(3)
O11	2*i*		0.079(2)	0.566(2)	0.877(2)	0.025(3)
O12	2*i*		0.100(2)	0.638(2)	0.545(2)	0.008(2)
O13	2*i*		0.218(2)	0.749(2)	0.796(2)	0.018(3)
O14	2*i*		−0.185(2)	0.305(2)	0.879(2)	0.020(3)
O1w	2*i*		0.202(2)	0.395(2)	0.011(2)	0.042(4)
O2w	2*i*		0.165(2)	0.120(2)	0.932(2)	0.033(4)
O3w	2*i*		0.143(2)	0.143(2)	0.186(2)	0.027(3)
O4w	2*i*		0.171(2)	0.153(2)	0.585(2)	0.033(4)
O5w	2*i*		0.360(2)	0.337(2)	0.488(2)	0.032(4)
O6w	2*i*		0.569(2)	0.554(2)	0.748(2)	0.026(3)
O7w	2*i*		0.380(2)	0.362(2)	0.838(2)	0.034(3)
OH1	2*i*		0.905(2)	0.287(2)	0.660(2)	0.015(3)
OH2	2*i*	0.5	0.541(4)	0.973(3)	0.000(3)	0.025(6)

Table 3
Anisotropic displacement parameters (Å^2) for metal atoms in $[Ni(H_2O)_4]_3[U(OH,-H_2O)(UO_2)_8O_{12}(OH)_3]$.

Atom	U_{11}	U_{22}	U_{33}	U_{12}	U_{13}	U_{23}
U1	0.0084(4)	0.0067(3)	0.0064(3)	0.0017(3)	0.0023(3)	0.0039(3)
U2	0.0081(4)	0.0075(3)	0.0048(3)	0.0015(3)	0.0021(3)	0.0034(3)
U3	0.0091(4)	0.0055(3)	0.0055(3)	0.0019(3)	0.0030(3)	0.0007(2)
U4	0.0082(4)	0.0076(3)	0.0096(3)	0.0019(3)	0.0039(3)	0.0058(3)
U5	0.046(1)	0.0185(6)	0.0054(5)	−0.0235(6)	0.0017(6)	0.0005(5)
Ni1	0.013(2)	0.014(2)	0.015(2)	0.006(2)	0.005(2)	0.009(1)
Ni2	0.027(2)	0.021(2)	0.013(2)	0.016(2)	0.006(2)	0.006(2)

temperature range 20–1000 °C, with a heating rate of 300° h^{-1}. Powder was placed in platinum crucibles.

3. Results

3.1. Cation coordination polyhedra

Table 4 contains selected interatomic distances and uranyl angles.

There are five symmetrically unique uranium atoms. Four of them, U(1), U(2), U(3) and U(4), are strongly bonded to two oxygen atoms forming nearly linear uranyl cations $(UO_2)^{2+}$ with a mean O═U═O bond-angle equal to 177.6(6)° and U═O bond-lengths ranging from 1.79(2) to 1.89(2) Å. That indicates unambiguously the presence of hexavalent uranium U(VI) at these sites. The average U═O value, 1.83(2) Å, is close to that of 1.79(3) Å calculated from uranyl polyhedra of numerous well-refined structures [17]. Of these, three [U(1), U(2) and U(3)]O_2^{2+} uranyl cations are further coordinated by four O atoms and one OH group (distinguished by valence bond calculations discussed below) located in the equatorial plane to form $[(UO_2)(OH)O_4]$ pentagonal bipyramids (Fig. 1). U(4) is coordinated by four oxygen atoms in the equatorial plane forming a $[(UO_2)O_4]$ square bipyramid. The equatorial U–O bond-lengths vary from 2.20(2) to 2.44(1) Å in $[(UO_2)(OH)O_4]$ pentagonal bipyramids, and from 2.20(2) to 2.25(9) Å in the $[(UO_2)O_4]$ square bipyramid. The average values, 2.32(2) and 2.23(6) Å, are in good agreement with the mean bond-lengths previously reported by Burns for $[U^{6+}O_7]$ and $[U^{6+}O_6]$ polyhedra [17], respectively. No uranyl bond was evidenced for U(5) atom. This atom is coordinated by four oxygen atoms at short distances (2.00(1) Å for two O(14) and 2.02(2) Å for two O(11)) leading to a distorted square. The coordination is completed by two water or hydroxyl oxygen atoms at longer distances (2.30(2) Å) forming a $[UO_4(OH,H_2O)]$ distorted octahedra. The mean U–O bond-length value, 2.11(2) Å, is quite similar to

Table 4
Selected interatomic distances (Å) and uranyl angles (°) for $[Ni(H_2O)_4]_3[U(OH,H_2O)(UO_2)_8O_{12}(OH)_3]$.

U1–O1	1.85(2)	U2–O3	1.79(2)
U1–O2	1.82(2)	U2–O4	1.81(2)
U1–O9^{ix}	2.291(9)	U2–O11	2.41(2)
U1–O9^{x}	2.26(2)	U2–O12	2.29(2)
U1–O10	2.34(2)	U2–O12^{iii}	2.21(1)
U1–O14^{xi}	2.44(1)	U2–O13	2.31(1)
U1–OH1	2.33(2)	U2–OH1^{xii}	2.35(2)
O1–U1–O2	178.0(4)	O3–U2–O4	177.1(7)
U3–O5	1.85(2)	U4–O7	1.89(2)
U3–O6^{iv}	1.80(2)	U4–O8	1.85(2)
U3–O10^{v}	2.22(1)	U4–O9	2.20(2)
U3–O11	2.41(2)	U4–O10^{viii}	2.225(9)
U3–O13	2.20(2)	U4–O12	2.249(9)
U3–O14^{vi}	2.42(2)	U4–O13	2.25(2)
U3–OH2^{iv}	2.30(3)	O7–U4–O8	177.5(5)
U3–OH2^{vii}	2.37(3)		
O5–U3–O6	177.7(9)		
U5–O11^{ii}	2.02(2)	Ni1–O2	2.03(2)
U5–O11^{iii}	2.02(2)	Ni1–O3	2.06(2)
U5–O14^{ii}	2.00(1)	Ni1–O4w	2.06(2)
U5–O14^{iii}	2.00(1)	Ni1–O5w	2.03(2)
U5–O1w	2.30(2)	Ni1–O6w	2.06(2)
U5–O1w^{i}	2.30(2)	Ni1–O7w	2.07(2)
Ni2–O2w^{ii}	2.14(2)	OH2–OH2^{xv}	1.02(5)
Ni2–O2w^{xiv}	2.14(2)		
Ni2–O3w	2.06(2)		
Ni2–O3w^{xiii}	2.06(2)		
Ni2–O6^{i}	2.00(2)		
Ni2–O6^{ix}	2.00(2)		

Symmetry codes: (i) −*x*, 1−*y*, −*z*; (ii) *x*, *y*, −1+*z*; (iii) −*x*, 1−*y*, 1−*z*; (iv) *x*, *y*, 1+*z*; (v) 1−*x*, 1−*y*, 2−*z*;(vi) −*x*, 1−*y*, 2−*z*; (vii) 1−*x*, 2−*y*, 1−*z*; (viii) *x*, 1+*y*, *z*; (ix) *x*, −1+*y*, *z*; (x) 1−*x*, 1−*y*, 1−*z*; (xi) 1+*x*, *y*, *z*; (xii) −1+*x*, *y*, *z*; (xiii) −*x*, −*y*, −*z*; (xiv) −*x*, −*y*, 1−*z*; AND (xv) 1−*x*, 2−*y*, −*z*.

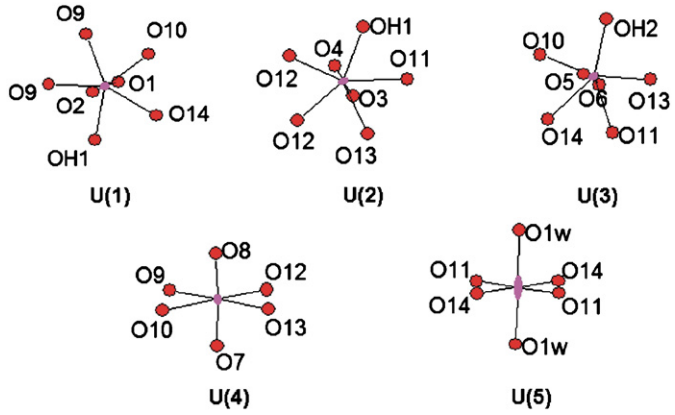

Fig. 1. Environment of the U atoms in $[Ni(H_2O)_4]_3[U(OH,H_2O)(UO_2)_8O_{12}(OH)_3]$.

Table 5
Bond valence sums for atoms in $[Ni(H_2O)_4]_3[U(OH,H_2O)(UO_2)_8O_{12}(OH)_3]$.

U(1) 5.98(7)	Ni(1) 2.04(3)
U(2) 6.27(7)	Ni(2) 1.98(4)
U(3) 6.1(1)	
U(4) 5.67(8)	
U(5) 5.57(7)	
O(1) 1.48(4)	O(1)w 0.62(2)
O(2) 1.92(5)	O(2)w 0.27(2)
O(3) 2.00(5)	O(3)w 0.33(1)
O(4) 1.58(5)	O(4)w 0.33(2)
O(5) 1.48(6)	O(5)w 0.36(2)
O(6) 2.01(7)	O(6)w 0.34(2)
O(7) 1.37(5)	O(7)w 0.32(2)
O(8) 1.48(5)	
O(9) 2.05(3)	OH(1) 1.15(2)
O(10) 2.01(3)	OH(2) 1.16(5)
O(11) 2.07(4)	
O(12) 2.04(3)	
O(13) 2.02(3)	
O(14) 2.07(3)	

that found for $[U^{6+}O_6]$ octahedron in $(NH_4)_3(UO_2)_2[(UO_2)_9O_{12}(OH)(H_2O)_2](H_2O)_2$ (2.09 Å), for example [18].

The two independent nickel atoms Ni(1) and Ni(2) are coordinated by two oxygen atoms and four H_2O groups forming nearly regular octahedra $[NiO_2(H_2O)_4]$ with Ni–O and Ni–OH_2 bond values ranging from 2.00(2) to 2.14(2) Å.

3.2. Chemical formula

The bond-valence sums were calculated using the coordination-independent parameters given by Burns et al. [19] for U–O bonds ($R_{ij} = 2.051$ Å, $b = 0.519$ Å) and the parameters given by Brown and Altermatt [20] for Ni–O bonds ($R_{ij} = 1.654$ Å, $b = 0.37$ Å). Calculations are in good agreement with hexavalent uranium U(VI) for U(1), U(2) and U(3) sites and with Ni^{2+} for Ni(1) and Ni(2) sites (Table 5). Obtained values do not allow, themselves, discriminating between (V) and (VI) valence states for U(4) and U(5) atoms (bond valence sums equivalent to ~5.6 *vu*). As U(4) pertains to an uranyl ion, its valence state is unambiguously hexavalent. In order to rule on the valence state for U(5), the bond-valence sums were compared to the data calculated for various structures. The bond valence sums calculated using the coordination-independent parameters for six coordinated hexavalent uranium evidence that they spread between 5.4 and 6.2 *vu*, with a maximum distribution occurring at 5.7 *vu* [19]. Higher bond-valence sums values for U(4) and U(5) (5.91(7) and 5.82(7) *vu*, respectively) are obtained by means of using the specific coordination parameters given by Burns et al. [19] for six coordinated hexavalent uranium, $R_{ij} = 2.074$ Å, $b = 0.554$ Å. Additionally, the average distances U–O (2.01 Å) and U–O(1)w (2.30 Å) of $[U(5)O_4(OH,H_2O)]$ distorted octahedra are significantly lower than the average U–O (2.15 Å) and U–OH_2 (2.42 Å) bond lengths calculated for pentavalent uranium containing oxides such as β-U_3O_8 [21], $NaUO_3$ [22], and $[U^V(H_2O)_2(U^{VI}O_2)_2O_4(OH)](H_2O)_4$ [23]. This is in agreement with the ionic radius shortening from pentavalent to hexavalent uranium. Therefore, the experimental values well support hexavalent uranium in U(5) sites. To confirm this hypothesis, a special attention was also paid to the calculation results at anion sites as previously detailed for various oxo-hydroxide compounds [10,11,24–33]. The results indicate there are 28 O^{2-} ions (O(1) to O(14) in general positions, bond valence sums within the range [1.37–2.07 *vu*]), three $(OH)^-$ groups (OH(1) and OH(2) in general position-half occupied for OH(2)-bond-valence sums ~1.15 *vu*) and twelve H_2O groups (O(2)w to O(7)w, bond-valence sums in the range [0.27–0.36 *vu*]). The bond-valence sums of O(1)w atom (0.62(2) *vu*) is intermediate between those of OH and H_2O oxygen atoms. Moreover, the U(5)–O(1)w distance (2.30(2) Å) is intermediate between the U^{6+}–OH distance in $Sr_5(UO_2)_{20}(UO_6)_2O_{16}(OH)_6(H_2O)_6$ [34] (2.25(2) Å) and the U^{6+}–OH_2 distance in $(NH_4)_3(UO_2)_2[(UO_2)_9O_{12}(OH)(H_2O)_2](H_2O)_2$ [18] (2.37(4) Å). So, it was concluded that O(1)w position is occupied by one oxygen atom belonging to a water molecule plus one another belonging to a hydroxyl ion leading to $[U^{6+}O_4(OH,H_2O)]$. The mixed occupancy of the U(5)–O(1)w site can explain the high anisotropic displacement parameter of the U(5) atom. Indeed, the anisotropic displacement ellipsoid elongated along the U(5)–O(1)w axis (Fig. 1) is the result of the displacement of the U(5) atom on each side of the mean plane toward the O(1)w atom leading to a shorter and a longer distance corresponding to the occupation of O(1)w site by OH and H_2O, respectively. That gives the structural formula $[Ni(H_2O)_4]_3[U(OH,H_2O)(UO_2)_8O_{12}(OH)_3]$ for the studied compound.

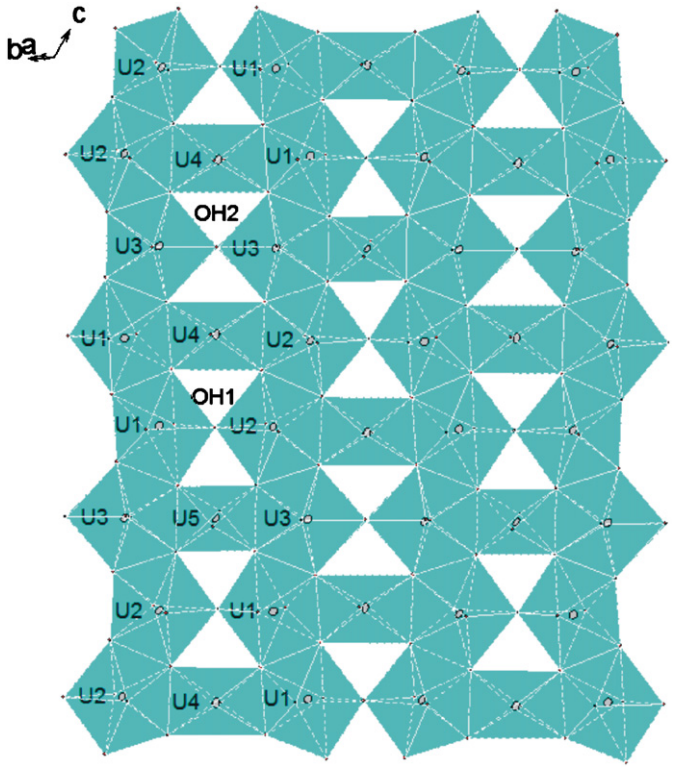

Fig. 2. The $[U(OH,H_2O)(UO_2)_8O_{12}(OH)_3]^{6-}$ sheets with the β-U_3O_8 anion-topology in $[Ni(H_2O)_4]_3[U(OH,H_2O)(UO_2)_8O_{12}(OH)_3]$.

3.3. Structural sheets of uranium polyhedra

As shown in Fig. 2, the crystal structure of $[Ni(H_2O)_4]_3[U(OH,H_2O)(UO_2)_8O_{12}(OH)_3]$ is based upon sheets of uranium polyhedra.

Fig. 3. The β-U_3O_8 (a) and α-U_3O_8 (e) sheet anion-topologies and the sheets obtained: (i) from β-U_3O_8 topology for O/OH = 14 in synthetic $(NH_4)_3(UO_2)_2[(UO_2)_9O_{12}(OH)(H_2O)_2](H_2O)_2$ [18] and $Sr_5(UO_2)_{20}(UO_6)_2O_{16}(OH)_6(H_2O)_6$ [34] (b), for O/OH = 4 in spriggite [11], $[U^V(H_2O)_2(U^{VI}O_2)_2O_4(OH)](H_2O)_4$ [23], ianthinite [24], wyartite [36], and synthetic $[Ni(H_2O)_4]_3[U(OH,H_2O)(UO_2)_8O_{12}(OH)_3]$ (present study) (c), (ii) from β or α topology for O/OH = 2/3 in ianthinite [24] (d), becquerelite [32] and compreignacite [27] (f), respectively. In billietite [33] the two types of sheets (e) and (f) coexist, and (iii) from α-U_3O_8 topology for O/OH = 3/2 in minerals masuyite [10], protasite [40], agrinierite [29], synthetic $Na_2[(UO_2)_3O_3(OH)_2]$ [31] (g) and in richetite [41] (h), for O/OH = 7/13 in $Cs_3[(UO_2)_{12}O_7(OH)_{13}]_2(H_2O)_3$ [28] (i). The position of (OH) groups is evidenced by circles.

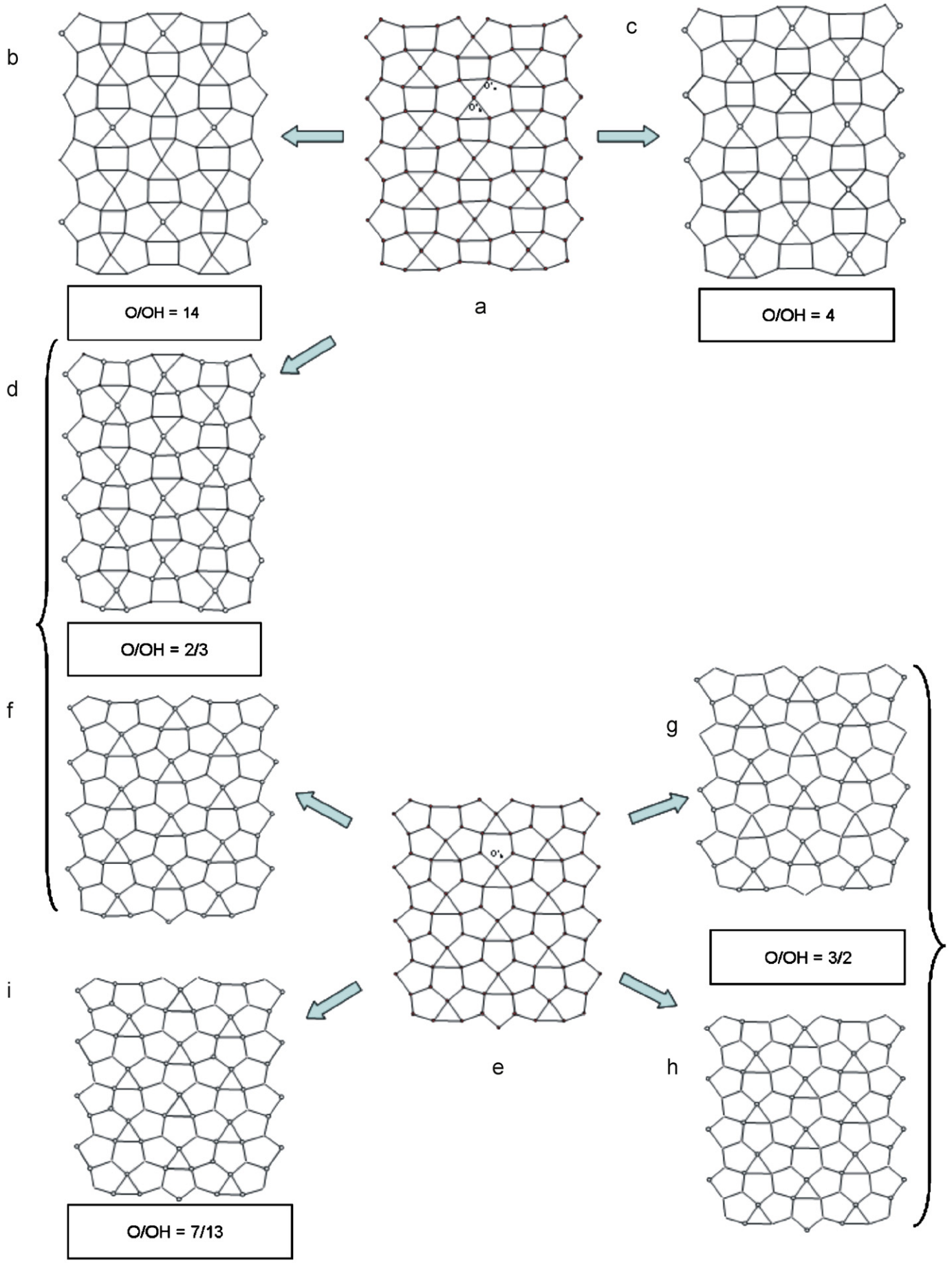
b
c
a
O/OH = 14
O/OH = 4
d
O/OH = 2/3
f
g
O/OH = 3/2
e
i
h
O/OH = 7/13

Table 6
Compositional data for some layered uranium-bearing oxo-hydroxide phases with structure derived from β and α-U_3O_8 sheets.

Compound	Site occupation				Sheet formula	O/OH	Anion topology	Ref.
β-U_3O_8	$^{[7]}(UO_2)_2$	$^{[6]}(UO_2)$	O'_{b}	O'_{a4}	$[(UO_2)_3O_5]^{4-}$	–	β-U_3O_8	[21]
$(NH_4)_3(UO_2)_2[(UO_2)_9O_{12}(OH)(H_2O)_2](H_2O)_2$[a]	$^{[7]}(UO_2)_2$	$^{[6]}(UO_2)_{2/3}$+$^{[6]}(U(H_2O)_2)_{1/3}$	$O_{2/3}(OH)_{1/3}$	O_4	$[(UO_2)_8U(H_2O)_2O_{14}(OH)]^{7-}$	14		[18]
$Sr_5(UO_2)_4[(UO_2)_{18}O_{24}(OH)_6](H_2O)_6$[a]	$^{[7]}(UO_2)_2$	$^{[6]}(UO_2)_{2/3}$+$^{[6]}(U(OH)_2)_{1/3}$	$O_{2/3}(OH)_{1/3}$	O_4	$[(UO_2)_8U(OH)_2O_{14}(OH)]^{9-}$	14		[34]
$[Ni(H_2O)_4]_3[U(OH,H_2O)(UO_2)_8O_{12}(OH)_3]$	$^{[7]}(UO_2)_2$	$^{[6]}(UO_2)_{2/3}$+$^{[6]}(U(OH)(H_2O))_{1/3}$	OH	O_4				
$[(UO_2)_8U(OH,H_2O)O_{12}(OH)_3]^{6-}$	4		Present work					
$Ca[U(UO_2)_2(CO_3)O_4(OH)](H_2O)_7$, wyartite	$^{[7]}(UO_2)_2$	$^{[6]}(U^{5+}(H_2O)(CO_3)$[b]$)$	OH	O_4				
$[(UO_2)_2U^{5+}(H_2O)(CO_3))O_4(OH)]^{2-}$	4		[36]					
$Pb_3[(UO_2)_6O_8(OH)_2](H_2O)_3$, spriggite	$^{[7]}(UO_2)_2$	$^{[6]}(UO_2)$	OH	O_4	$[(UO_2)_3O_4(OH)]^{3-}$	4		[11]
$[U^{5+}(UO_2)_2O_4(OH)(H_2O)_2](H_2O)_4$	$^{[7]}(UO_2)_2$	$^{[6]}[U^{5+}(H_2O)_2]$	OH	O_4	$[U^{5+}(UO_2)_2O_4(OH)(H_2O)_2]$	4		[23]
$[U^{4+}_2(UO_2)_4O_6(OH)_4(H_2O)_4](H_2O)_5$, ianthinite	$^{[7]}(UO_2)_2$	$^{[6]}(U^{4+}(H_2O)_2)$	OH	O_4	$[(UO_2)_2U^{4+}(H_2O)_2O_4(OH)]^{-}$	4		[24]
				$O_2(OH)_2$	$[(UO_2)_2U^{4+}(H_2O)_2O_2(OH)_3]^{+}$	2/3		
$Ba[(UO_2)_6O_4(OH)_6](H_2O)_8$, billietite	$^{[7]}(UO_2)_2$	$^{[6]}(UO_2)$	OH	$O_2(OH)_2$	$[(UO_2)_3O_2(OH)_3]^{-}$	2/3	β-U_3O_8	[33]
		$^{[7]}(UO_2)$	OH	$O_2(OH)_2$	$[(UO_2)_3O_2(OH)_3]^{-}$	2/3	α-U_3O_8	
α-U_3O_8	$^{[7]}(UO_2)_2$	$^{[7]}(UO_2)$	O'_{b}	O'_{a4}	$[(UO_2)_3O_5]^{4-}$	–	α-U_3O_8	[38,39]
$Pb[(UO_2)_3O_3(OH)_2](H_2O)_3$, masuyite	$^{[7]}(UO_2)_2$	$^{[7]}(UO_2)$	OH	$O_3(OH)_1$	$[(UO_2)_3O_3(OH)_2]^{2-}$	3/2		[10]
$Ba[(UO_2)_3O_3(OH)_2](H_2O)_3$, protasite								[40]
$Na_2[(UO_2)_3O_3(OH)_2]$								[31]
$K_2(Ca_{0.65}Sr_{0.35})[(UO_2)_3O_3(OH)_2]_2(H_2O)_5$, agrinierite								[29]
$(Fe,Mg)_xPb_{8.57}[(UO_2)_{18}O_{18}(OH)_{12}]_2(H_2O)_{41}$, richetite	$^{[7]}(UO_2)_2$	$^{[7]}(UO_2)$	$O_{1/3}(OH)_{2/3}$	$O_{8/3}(OH)_{4/3}$	$[(UO_2)_3O_3(OH)_2]^{2-}$	3/2		[41]
$Ca[(UO_2)_3O_2(OH)_3]_2(H_2O)_8$, becquerelite	$^{[7]}(UO_2)_2$	$^{[7]}(UO_2)$	OH	$O_2(OH)_2$	$[(UO_2)_3O_2(OH)_3]^{-}$	2/3		[32]
$K_2[(UO_2)_3O_2(OH)_3]_2(H_2O)_7$, compreignacite								[27]
$Cs_3[(UO_2)_{12}O_7(OH)_{13}]_2(H_2O)_3$	$^{[7]}(UO_2)_2$	$^{[7]}(UO_2)$	OH	$O_{7/4}(OH)_{9/4}$	$[(UO_2)_3O_{7/4}(OH)_{3/4}]^{3/4-}$	7/13		[28]

[a] In these compounds, UO_2^{2+} uranyl ions occupy the interlayer space. Their coordination are completed by one O'_b atom and four oxo atoms O of $^{[7]}(UO_2)_2$ ions to form $[UO_7]$ pentagonal bipyramids pillaring the sheets to built an open framework.
[b] One oxygen atom is replaced by two oxygen atoms of one carbonate group which acts as bidentate.

The $[(UO_2)(OH)O_4]$ pentagonal bipyramids of the sheets share O–O equatorial edges to form $^1_\infty[UO_5]$ chains running perpendicularly to the b axis with the sequence –(U(1)–U(1)–U(3)–U(2)–U(2)–U(3))–. Adjacent chains are directly connected by the hydroxyl groups OH(1) and OH(2) shared between two U(3) atoms and between U(1) and U(2) atoms, respectively. Adjacent chains are also cross-linked by $[(U(4)O_2)O_4]$ and $[U(5)O_4(OH)(H_2O)]$ square bipyramids. OH(2) site (general 2*i* Wyckoff position) is disordered and half occupied on both side of the mean plane of the sheet. Such a disorder of the shared OH groups was previously observed in $Sr_5(UO_2)_{20}(UO_6)_2O_{16}(OH)_6(H_2O)_6$ [34] containing the same type of uranium sheets. This structural arrangement results in sheets with the β-U_3O_8 anion-topology [17,35] (Fig. 3a) in which all the pentagons and the squares are occupied by uranium while the triangles are empty as in β-U_3O_8 [21] and in closely related compounds such as ianthinite, $[U^{4+}_2(UO_2)_4O_6(OH)_4(H_2O)_4](H_2O)_5$ [24], spriggite $Pb_3((UO_2)_6O_8(OH)_2)(H_2O)_3$ [11], $(NH_4)_3(UO_2)_2[(UO_2)_9O_{12}(OH)(H_2O)_2](H_2O)_2$ [18], $Sr_5(UO_2)_{20}(UO_6)_2O_{16}(OH)_6(H_2O)_6$ [34] and in the structurally related wyartite, $Ca[U_2(UO_2)_2(CO_3)O_4(OH)(H_2O)](H_2O)_6$ [36]. As can be seen from Figs. 3a–d, the β-U_3O_8 structural arrangement allows substituting $O^{2-} \leftrightarrow OH^-$. In $[Ni(H_2O)_4]_3[U(OH,H_2O)(UO_2)_8O_{12}(OH)_3]$, the sheet composition, $[U(OH,H_2O)(UO_2)_8O_{12}(OH)_3]$, corresponds to a O^{2-}/OH^- ratio equal to 4:1. This ratio is identical to the one found in spriggite [11], ianthinite [24], $[U^V(H_2O)_2(U^{VI}O_2)_2O_4(OH)](H_2O)_4$ [23] and wyartite [36]. The OH^- groups distribution within these layers leads all the bow-tie-like motifs to be connected centrally by hydroxyl groups (Fig. 3c).

3.4. Analysis of the distribution of hydroxyl groups

The most common method for reporting formulas of oxo-hydroxide hydrates does not include the positions of the apical or equatorial OH and H_2O groups within the layers themselves. Herein, an attempt to rewrite the formulas of some oxo-hydroxide hydrates was undertaken with the aim to emphasize the distribution of OH and H_2O groups and to study the influence of the O/OH content on the structural arrangement of the sheets. To do so, a formalism based on the β-U_3O_8 type sheets was used. The β-U_3O_8 type sheets contain hexavalent uranium in pentagonal bipyramids, which are uranyl part $^{[7]}UO_2$, and uranium cations with multiple valence states, U^{6+}, U^{5+} or U^{4+} which are in square bipyramids noted $^{[6]}UO_2$. The $^{[7]}UO_2/^{[6]}UO_2$ is equal to 2. In β-U_3O_8, the sheets can be formulated $^2_\infty[(^{[7]}UO_2)_2(^{[6]}UO_2)O'_5]$ where O denotes apical oxygen atoms and O′ denotes equatorial oxygen atoms shared between the uranium polyhedra of the sheets. Two types of oxygen atoms O′ can be distinguished, the oxygen atoms shared between pentagonal and square bipyramids, denoted O'_a, and the oxygen atoms shared between $^1_\infty[UO_5]$ chains, denoted O'_b (Fig. 3a). In the β-U_3O_8 structurally related compounds, either only O'_b are replaced by hydroxyl oxygen atoms (Fig. 3b and c)-but also by chlorine atoms as in $M_7(UO_2)_8(VO_4)_2O_8Cl$, M = Rb, Cs [37], for example-or both O'_a and O'_b (Fig. 3d). So, the β-U_3O_8 type-sheets should be formulated $^2_\infty[^{[7]}(UO_2)_2{}^{[6]}(UO_2)O'_{a4}O'_b]$ in order to evidence the structural relationships between the β-U_3O_8 type compounds. The net charge of the sheets can be modified by (i) distinct distributions of OH groups on O'_b and O'_a sites, (ii) replacement of O atoms of $^{[6]}(UO_2)$ entities by OH or H_2O oxygen atoms, (iii) replacement of hexavalent uranium of $^{[6]}(UO_2)$ entities by U(V) or U(IV). Using this formalism leads to the structural formula reported Table 6. According to the O/OH ratio within the sheets, three distributions of hydroxyl oxygen atoms can be distinguished for the β-U_3O_8 type-sheets (Fig. 3). They correspond to O/OH ratio equal to 14 in synthetic $(NH_4)_3(UO_2)_2[(UO_2)_9O_{12}(OH)(H_2O)_2](H_2O)_2$ [18] and $Sr_5(UO_2)_{20}(UO_6)_2O_{16}(OH)_6(H_2O)_6$ [34] (Fig. 3b), to O/OH ratio = 4 in spriggite [11], ianthinite [24], $[U^V(H_2O)_2(U^{VI}O_2)_2O_4(OH)](H_2O)_4$ [23], wyartite [36], and synthetic $[Ni(H_2O)_4]_3[U(OH,H_2O)(UO_2)_8O_{12}(OH)_3]$ (Fig. 3c) and to O/OH ratio = 2/3 in ianthinite [24] and billietite [33] (Fig. 3d). In

the latter, 1/3 of the bow-tie-like motifs are connected by doubly bridging OH groups although in the former all the corners of triangles are occupied by OH groups.

In many other compounds, distortion of the $^{1}_{\infty}[UO_5]$ chains allows integrating O'_b atoms into the coordination polyhedra of uranium that goes from square to pentagonal bipyramidal environment. A square and a triangle of the β-U_3O_8 sheet anion-topology are then transformed into a pentagon to generate the α-U_3O_8 sheet anion-topology (Fig. 3e) as found in α-U_3O_8 [38,39] and in various oxo-hydroxides hydrates compounds. As observed for the β-U_3O_8 structurally related compounds, various O/OH distributions led to four different layers found (i) in becquerelite [32], compreignacite [27] and billietite [33] (O/OH = 2/3-Fig. 3f) (ii) in masuyite [10], protasite [40], agrinierite [29], synthetic $Na_2[(UO_2)_3O_3(OH)_2]$ [31] (O/OH = 3/2—Fig. 3(g), (iii) in richetite [41] (O/OH = 3/2—Fig. 3(h) and (iv) in synthetic $Cs_3[(UO_2)_{12}O_7(OH)_{13}](H_2O)_3$ [28] (O/OH = 7/13—Fig. 3i).

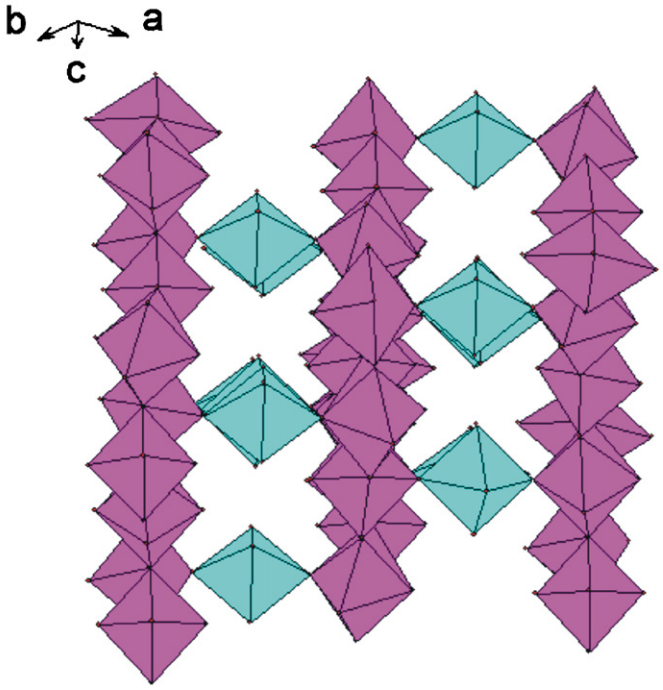

Fig. 4. The framework built from uranium polyhedra sheets pillared by Ni-centered octahedra.

Applying the as-described formalism to oxo-hydroxide hydrates evidences that α-U_3O_8 is rather obtained for lower O/OH ratio (Table 6). Furthermore, uranium is always fully oxidized in the α-U_3O_8 structurally related oxo-hydroxides whereas the various oxo-hydroxide compounds related to the β-U_3O_8 anion-topology allow accommodating multiple valence states of uranium such as (U(IV)/U(VI)) in ianthinite [24] and (U(V)/U(VI)) in wyartite [36] and in $[U^{V}(H_2O)_2(U^{VI}O_2)_2O_4(OH)](H_2O)_4$ [23].

3.5. Interlayer connectivity

Whatever the anion-topology of the considered oxo-hydroxides, $O^{2-} \leftrightarrow OH^-$ substitutions can be accompanied by additional charge-balancing. That occurs by incorporating additional interlayer low-valence cations. In the compound reported herein, the anionic charge of the $[U(OH,H_2O)(UO_2)_8O_{12}(OH)_3]^{6-}$ sheets is compensated by Ni^{2+} interlayer cations surrounded by four water molecules. The coordination of Ni^{2+} is completed by two oxygen atoms which belong to UO_2^{2+} ions of the uranium polyhedra layers. Successive layers are linked together by two perpendicular metal–oxygen links: O(1)═U(1)═O(2)–Ni(1)–O(3)═U(2)-═O(4) and O(5)═U(3)═O(6)–Ni(2)–O(6)═U(3)═O(5). So, the uranyl polyhedra sheets can be considered as pillared by $NiO_2(H_2O)_4$ octahedra to form a three-dimensional framework (Fig. 4) creating empty tunnels.

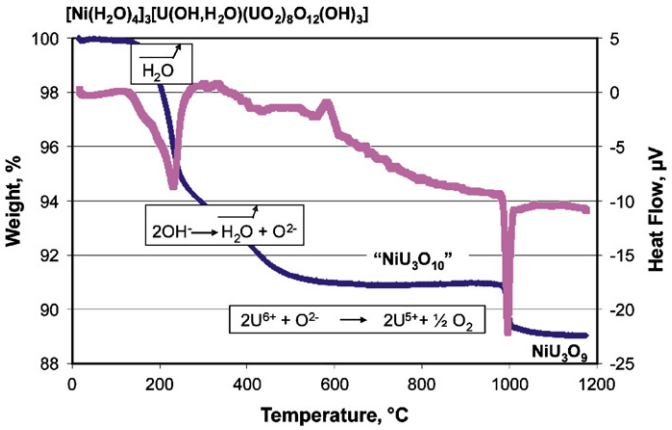

Fig. 6. TGA/TDA/MS curves for $[Ni(H_2O)_4]_3[U(OH,H_2O)(UO_2)_8O_{12}(OH)_3]$ under

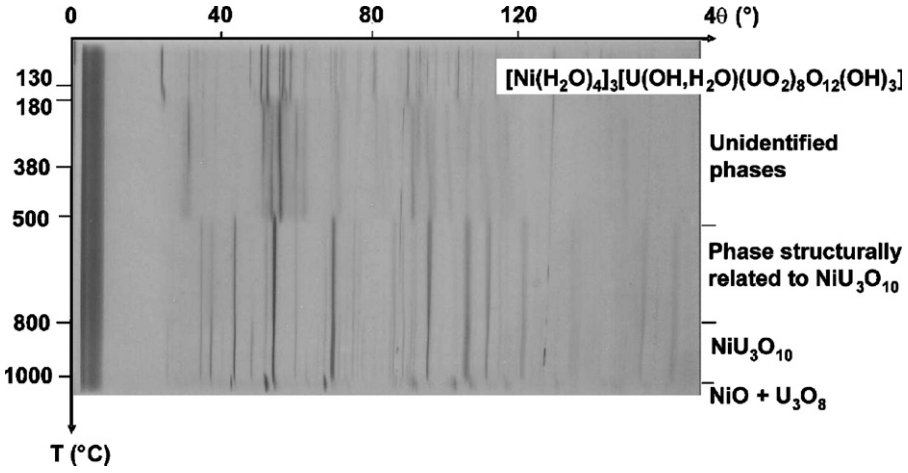

Fig. 5. HTXRD Guinier-Lenné pattern for $[Ni(H_2O)_4]_3[U(OH,H_2O)(UO_2)_8O_{12}(OH)_3]$ in air (heating rate ~0.4° min^{-1}). flowing air (heating rate: 5° min^{-1}).

3.6. Thermal behavior

High-temperature X-ray diffraction evidences that the thermal decomposition of $[Ni(H_2O)_4]_3[U(OH,H_2O)(UO_2)_8O_{12}(OH)_3]$ is accompanied by changes within the X-ray diffraction patterns. No intermediate phase could be identified using the PDF database, except that the starting compound is transformed into NiU_3O_{10} (PDF 44-0978) [42–44] at 800 °C, (Fig. 5). TGA/DTA experiments (Fig. 6) confirm that the thermal decomposition of $[Ni(H_2O)_4]_3[U(OH,H_2O)(UO_2)_8O_{12}(OH)_3]$ occurs in several steps, as follows.

The first mass-loss within the range of temperature [130–800 °C] (exp. 9.0%) is in good agreement with the dehydration and dehydroxylation of $[Ni(H_2O)_4]_3[U(OH,H_2O)(UO_2)_8O_{12}(OH)_3]$ (theor. 8.8%). That leads to an intermediate phase structurally related to NiU_3O_{10} and observed on X-ray diffraction patterns between 500 and 800 °C.

The second mass loss at 1000 °C was previously attributed to the transformation of NiU_3O_{10} into NiU_3O_9 [42,43]. Our TGA/DTA experiments confirm this conclusion in that the calculated value based upon the reaction $2U^{6+}+O^{2-}\rightarrow 2U^{5+}+1/2O_2$ (theor. 1.7%) perfectly agrees with the experimental value (exp. 1.8%). However, after quenching in air from 1000 °C, decomposition of this phase into NiO and U_3O_8 is observed (Fig. 5).

4. Conclusion

Reacting uranyl and nickel nitrates with an excess of oxalic acid by means of hydrothermal synthesis allows obtaining $[Ni(H_2O)_4]_3[U(OH,H_2O)(UO_2)_8O_{12}(OH)_3]$. The neutral framework of the compound is built from anionic sheets with formula $[[U(OH,H_2O)(UO_2)_8O_{12}(OH)_3]^{6-}$, which are charge balanced by additional interlayer $[Ni(H_2O)_4]^{2+}$ cations. The sheets adopt the flexible β-U_3O_8 anion-topology, which allows various $O^{2-}\leftrightarrow OH^-$ substitutions and replacement of some uranyl ions by U^{6+} or lower valent uranium such as U^{4+} and U^{5+}. In $[Ni(H_2O)_4]_3[U(OH,H_2O)(UO_2)_8O_{12}(OH)_3]$, the sheets are built from chains of edge-shared $[(UO_2)(OH)O_4]$ pentagonal bipyramids connected through $[U^{6+}O_4(H_2O)(OH)]$ and $[(UO_2)O_4]$ square bipyramids. The sheets are pillared by $[NiO_2(H_2O)_4]$ octahedra to form a three-dimensional framework with empty channels. The thermal decomposition of $[Ni(H_2O)_4]_3[U(OH,H_2O)(UO_2)_8O_{12}(OH)_3]$ leads to the stabilization of the NiU_3O_{10} phase in the temperature range [800–1000 °C]. After quenching from 1000 °C, a decomposition of the final product into NiO and U_3O_8 is evidenced.

Acknowledgments

The "Fonds Européen de Développement Régional (FEDER)", "CNRS", "Région Nord Pas-de-Calais" and "Ministère de l'Education Nationale de l'Enseignement Supérieur et de la Recherche" are acknowledged for fundings of X-ray diffractometers.

The crystallographic data are deposited and can be obtained through the FIZ data bank.

Appendix A. Supplementary data

Supplementary data associated with this article can be found in the online version at doi:10.1016/j.jssc.2009.01.019.

References

[1] R.J. Finch, R.C. Ewing, J. Nucl. Mater. 190 (1992) 133.
[2] L.H. Johnson, L.O. Werme, Mater. Res. Soc. Bull. XIX (12) (1994) 24.
[3] R.S. Forsyth, L.O. Werme, J. Nucl. Mater. 190 (1992) 3.
[4] D.J. Wronkiewicz, J.K. Bates, T.J. Gerding, E. Veleckis, B.S. Tani, J. Nucl. Mater. 190 (1992) 107.
[5] T. Wadsten, J. Nucl. Mater. 64 (1977) 315.
[6] R. Vochten, L. Van Haverbeke, R. Sobry, J. Mater. Chem. 1 (4) (1991) 637.
[7] H. Brasseur, Bull. Soc. Fr. Miner. Cryst. 85 (1962) 242.
[8] R.J. Finch, M.A. Cooper, F.C. Hawthorne, Can. Mineral. 34 (1996) 1071.
[9] P.C. Burns, R.C. Ewing, M.L. Miller, J. Nucl. Mater. 245 (1997) 1.
[10] P.C. Burns, J.M. Hanchar, Can. Mineral. 37 (1999) 1483.
[11] J. Brugger, S.V. Krivovichev, P. Berlepsch, N. Meisser, S. Ansermet, T. Armbruster, Am. Mineral. 89 (2004) 339.
[12] G.M. Scheldrick, CELL_NOW-Version 2008-2-Index Twins and Other Problem Crystals, Goetingen, Germany, 2008.
[13] SAINT plus Version 7.53a, Bruker Analytical X-ray Systems, Madison, WI, 2008.
[14] G.M. Scheldrick, TWINABS-Bruker AXS scaling for twinned crystals-Version 2008/1, Goetingen, Germany, 2008.
[15] V. Petricek, M. Dusek, L. Palatinus, JANA2000, Institute of Physics, Praha, Czech Republic, 2005.
[16] A. Altomare, G. Cascaro, G. Giacovazzo, A. Guargliardi, M.C. Burla, G. Polidori, M. Gamalli, J. Appl. Crystallogr. 27 (1994) 135.
[17] P.C. Burns, Can. Mineral. 43 (2005) 1839.
[18] Y. Li, C.L. Cahill, P.C. Burns, Chem. Mater. 13 (2001) 4026.
[19] P.C. Burns, R.C. Ewing, F.C. Hawthorne, Can. Mineral. 35 (1997) 1551.
[20] I.D. Brown, D. Altermatt, Acta Cryst. B 41 (1985) 244.
[21] B.O. Loopstra, Acta Crystallogr. B 26 (1970) 656.
[22] A.M. Chippindale, P.G. Dickens, W.T.A. Harrison, J. Solid State Chem. 78 (1989) 256.
[23] N. Belai, M. Frisch, E.S. Ilton, B. Ravel, C.L. Cahill, Inorg. Chem. 47 (2008) 10135.
[24] P.C. Burns, R.J. Finch, F.C. Hawthorne, M.L. Miller, R.C. Ewing, J. Nucl. Mater. 249 (1997) 199.
[25] P. Piret, Bull. Miner. 108 (1985) 659.
[26] R.J. Finch, M.A. Cooper, F.C. Hawthorne, Can. Mineral. 34 (1996) 1071.
[27] P.C. Burns, Can. Mineral. 36 (1998) 1061.
[28] F.C. Hill, P.C. Burns, Can. Mineral. 37 (1999) 1283.
[29] C.L. Cahill, P.C. Burns, Am. Mineral. 85 (2000) 1294.
[30] M.T. Weller, M.E. Light, T. Gelbrich Acta Cryst. B 56 (2000) 577.
[31] Y. Li, P.C. Burns, J. Nucl. Mater. 299 (2001) 219.
[32] P.C. Burns, Y. Li, Am. Mineral. 87 (2002) 550.
[33] R.J. Finch, P.C. Burns, F.C. Hawthorne, R.C. Ewing, Can. Mineral. 44 (2006) 1197.
[34] K.-A. Kubatko, P.C. Burns, Inorg. Chem. 45 (2006) 10277.
[35] P.C. Burns, M.L. Miller, R.C. Ewing, Can. Mineral. 34 (1996) 845.
[36] P.C. Burns, R.J. Finch, Am. Mineral. 84 (1999) 1456.
[37] I. Duribreux, M. Saadi, S. Obbade, C. Dion, F. Abraham, J. Solid State Chem. 172 (2003) 351.
[38] B.O. Loopstra, Acta Crystallogr. 17 (1964) 651.
[39] B.O. Loopstra, J. Appl. Crystallogr. 3 (1970) 94.
[40] M.K. Pagoaga, D.E. Appleman, J.M. Stewart, Am. Mineral. 72 (1987) 1230.
[41] P.C. Burns, Can. Mineral. 46 (1998) 187.
[42] C. Brisi, Ann. Chim. 53 (1963) 325.
[43] W.L. Marshall, J.S. Gill, J. Inorg. Nucl. Chem. 26 (1964) 277.
[44] V. Serezhkin, Radiokhimiya 23 (1981) 392.